

# VCSEL-based, CWDM - PON systems using reflective technology for bi-directional multi-play service provision

Terence Quinlan,<sup>1,\*</sup> Sandra Dudley,<sup>2</sup> Maria Morant,<sup>3</sup> Roberto Llorente,<sup>3</sup>  
and Stuart Walker<sup>1</sup>

<sup>1</sup> School of Computer Science and Electronic Engineering, University of Essex, CO4 3SQ Colchester, UK

<sup>2</sup> Engineering and Design department, London South bank University, 103 Borough Road, London, UK

<sup>3</sup> Valencia Nanophotonics Technology Centre, Universidad Polit cnica de Valencia, 46022 Valencia, Spain  
[quinlan@essex.ac.uk](mailto:quinlan@essex.ac.uk)

**Abstract:** Orthogonal frequency division multiplexing based on radio-over-fiber schemes allows the direct use of multiple, native format wireless platforms. In combination with standard baseband provision such as Gigabit Ethernet, this provides access to a wide range of services without requiring specialized end-user equipment. However, such signals have a high laser power-bandwidth requirement which may not be a good fit to the domestic environment. Here we explore the use of low-power optical components in customer premises which interface with an intermediate optical network node. Two solutions in the context of SSMF over a CWDM optical network are described, based on either reflective or direct modulation. EVMs of better than  $-35$  dB were achieved.

 2012 Optical Society of America

**OCIS codes:** (060.0060) Fiber optics and optical communications; (060.1155) All-optical networks.

---

## References and links

1. J. Guillyory, A. Pizzinat, P. Guignard, F. Richard, B. Charbonnier, C. Algani, and P. Chanclou. "Simultaneous implementation of gigabit ethernet, RF TV and radio mm-wave in a multiformat home area network," in proceedings of ECOC (2011), paper We.7.C.3.
2. M. Morant, T. Quinlan, R. Llorente, and S. Walker, "Full standard triple-play bi-directional and full-duplex CWDM transmission in passive optical networks," in proceedings OFC (2011), paper OWB3.
3. M. Morant, T. Quinlan, S. Walker, and R. Llorente, "Complete mitigation of brillouin scattering effects in reflective passive optical networks using triple-format OFDM radio signals," in proceedings OFC (2011), paper JWA072.
4. T. Quinlan, S. Dudley, M. Morant, R. Llorente, and S. Walker, "First demonstration of cooler-less, bi-directional, format-agnostic, wireless and gigabit ethernet network provision using off-the-shelf VCSELs," in proceedings OFC (2012), paper OTh3G.1.
5. M. V. R. Murty, X. D. Huang, G. L. Liu, C. C. Lin, D. Xu, C. L. Shieh, H. C. Lee, and J. Cheng, "Long-wavelength VCSEL-based CWDM scheme for 10-GbE links," *IEEE Photon. Technol. Lett.* **17**(6), 1286–1288 (2005).
6. 3GPP TS 36.101 V8.8.0 "3rd Generation Partnership Project; technical specification group radio access network; Evolved universal terrestrial radio access (E-UTRA); User equipment (UE) radio transmission and reception (Release 8)," (2009).
7. IEEE 802.16 Standard for local and metropolitan area networks "Part 16: Air interface for fixed broadband wireless access systems," (2009).
8. ECMA-368, "High rate ultra-wideband PHY and MAC standard," ECMA Int. (2007).

---

## 1. Introduction

There is much interest currently being focused on commercial, off-the-shelf technology for delivery of wireless signals such as ultra-wide band (UWB), WiMAX, LTE and baseband signals including Gigabit Ethernet (GbE) over legacy standard single mode fiber (SSMF) e.g [1]. Using standard off-the-shelf components it has been shown that coarse wavelength division multiplexed (CWDM) schemes are capable of transmitting multiple wireless formats bi-directionally over at least 75 km of fiber [2]. However, the lasers used at the customer

premises require cooling and are relatively high powered ( $> +10$  dBm). CWDM used at these distances also compromises power distribution in the 1300 nm region. The introduction of an intermediate node allows the use of standard central exchange wavelength division multiplexing (WDM); with the final span deploying low power devices in CWDM format to the end user premises. The use of low power devices offers distinct advantages to the service provider where power consumption at remote nodes is a critical factor. Also, in the domestic environment, customer safety is an overriding consideration. Reflective and directly modulated low power devices such as those described, fulfill these requirements whilst enabling simplicity of deployment. Two methods for fiber to the home service delivery were considered, with a target range of 20 km based on the concept shown in Fig. 1.

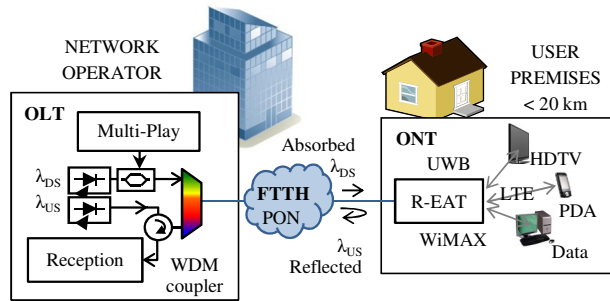


Fig. 1. Reflective bi-directional network based on R-EAT for multi-play service provision

We evaluated experimentally the ability of each one to deliver simultaneously three OFDM based wireless formats (LTE, WiMAX, and WiMedia UWB), and a digital baseband signal in both upstream (US) and downstream (DS) direction. Firstly a reflective system was assessed; where a reflective electro-absorption transducer (R-EAT) was situated in the customer premises [3]. The R-EAT is effectively a linearized reflective electro-absorption modulator (R-EAM) where a degree of sensitivity is sacrificed in return for increased linearity. This device operated as a reflective modulator at 1500nm and as an absorptive detector at 1300nm wavelengths. Such an arrangement permitted both US and DS lasers to be remotely sited and therefore ideal for customer premises provision. These devices were capable of operation over a wide RF bandwidth and were sufficiently linear to handle OFDM-based wireless formats. Nevertheless, this was not an ideal solution as full duplex transmission was not possible. A common US/DS radio frequency connection was necessary within the device which required switching. Additionally, the digital baseband RF spectrum was degraded by stimulated Brillouin Scattering (SBS) products. In the second system to be assessed, a standard CWDM architecture was utilized. Directly modulated, off-the-shelf VCSELs provided sufficient bandwidth for Radio over Fiber (RoF) signals  $> 5$  GHz [4]; with a conventional photodiode and RF amplifier arrangement completing the system. This arrangement provided US/DS isolation  $> 40$  dB together with a full duplex capability as there are simultaneous paths in opposite directions at 1345.6 nm and 1541.9 nm. The low component count features of such a PON also offered reduced cost with standard equipment used at both ends of the architecture. Whilst output power and wavelength temperature dependence were not a primary concern (typically  $46 \mu\text{W/K}$  and  $80 \text{ pm/K}$  respectively [5]), wavelength current perturbation was a serious concern at typically  $0.3 \text{ nm/mA}$  [5], allowing only cooler-less CWDM applications. As with the R-EAT solution, 480 Mbit/s band-group 1 (3.168 GHz to 4.752 GHz) UWB, WiMAX and LTE were supported at EVM levels within the standards requirement of  $-18$  dB for GPP LTE using 16QAM [6],  $-24.43$  dB for 802.16 WiMAX using 16QAM [7], and  $-17$  dB for ECMA-368 UWB using DCM [8]. In addition, the directly modulated solution permits a bi-directional  $> 2$  Gbps baseband channel, supporting Gigabit Ethernet. Looking ahead, using latest-generation LTE, 802.11ad, 802.11ac or emerging 802.11ah wireless services, WiFi or 60 GHz ISM band pico-cell connectivity

could be implemented for hub-to-home and in building fixed/mobile distribution. 802.11ac is set to offer multi-user MIMO and beam-forming capability at predicted capacities of 1.3 Gbit/s (plus 450 Mbit/s legacy). The putative offer of GbE to the home via wireless has been considered on many previous occasions but this scenario is now closer. Both schemes offer RoF range extension to 100km or beyond with a user friendly domestic optical interface. The ability of standard wireless formats to co-exist with baseband signals in this environment creates a flexible “band agnostic” transmission system.

## 2. Reflective experimental system

The experimental system is shown in Fig. 2(a). Three wireless formats were constructed using two Agilent E4438C arbitrary waveform generators and a Wisair UWB dongle. These formats consisted 16QAM LTE at 2.6 GHz with 20 MHz bandwidth 16QAM WiMAX at 3.5 GHz at 24 MHz bandwidth and a band 1, 480 Mbps WiMedia UWB signal set for time - frequency code TFC6 (at 3.96 GHz center frequency), in 528 MHz bandwidth. These signals were then combined using a Wilkinson-type RF combiner (Mini-Circuits ZN4PD1-50) with typically 6.9 dB insertion loss. At this stage, optimization of the power levels in each format was required, so minimizing EVM variation; this procedure accounted for the burst nature of the signals to ensure that all three formats are present at the time of analysis. As shown in Fig. 2(b), the resulting spectrogram indicated the simultaneous presence of the signal whilst Fig. 2(c) shows the resulting spectrum and the relative power levels. Figure 2(d) shows the ensuing constellations under launch conditions. This signal was then used to drive the Mach-Zehnder Modulator (Covega LN-058).

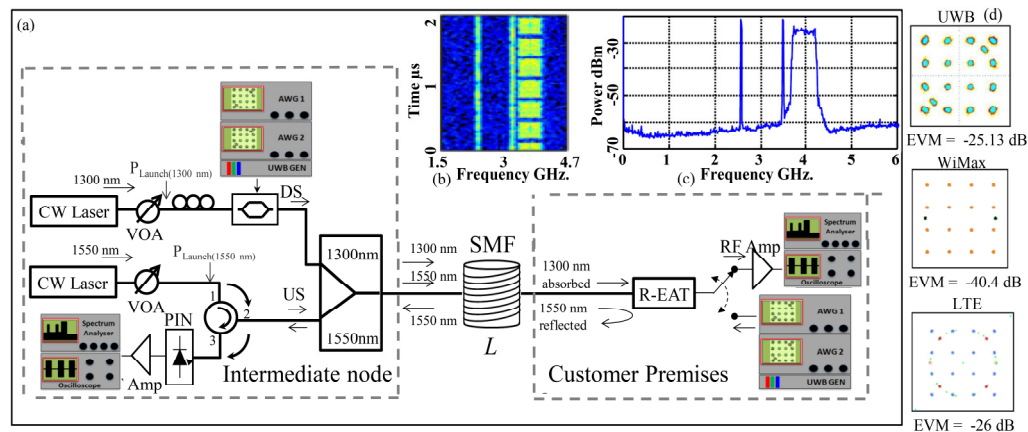


Fig. 2. (a) Reflective system experimental setup. (b) Spectrogram of combined formats at launch. (c) Frequency spectrum at launch. (d) Respective constellations and measured EVM at launch

The DS optical path consisted of a 1345 nm laser (DFB-1310-BF-31-CW-FC-537) with a power output of 14.5 dBm feeding into a Mach-Zehnder modulator via an optical attenuator and polarization controller. At this point, a CWDM splitter was used to connect the set-up to a length of SSMF) and on to the R-EAT. This arrangement was then adjusted to optimum bias for best quality reception at the R-EAT sited at the user premises. Here, a Hittite RF switch (HMC270) was used to separate US and DS conditions. The resulting signal was then amplified by 56 dB and then analyzed using a Tekronix DPO 71254 oscilloscope and an Agilent EXA N9010A spectrum analyzer. In the US optical path, a 1541 nm (Fitel FOL15DCWD-A81-19270-B) laser, also at a power level of 14.5 dBm was applied to port 1 of a circulator. As before, an optical attenuator was inserted at this point to provide optimal conditions at the R-EAT. Port 2 of the circulator was then connected to the 1500 nm arm of the CWDM splitter which in turn provided the reflective channel to the R-EAT. At this node, the R-EAT was directly modulated by an identically generated multi-format wireless signal

(via the RF switch), thus generating the US signal. This reflected information then returned via ports 2 & 3 of the circulator to a Discovery 10 GHz bandwidth DSC-R402AC photodiode after which it was again subject to 56 dB amplification and then analyzed. Signal quality was evaluated after propagation through differing lengths of SSMF to establish the maximum reach of the system. This maximum reach limit was obtained by comparing the measured EVM in each path to that of the EVM limits as set out in the appropriate current radio standards. Although this set-up process required extensive experimental investigation, the situation for large-scale deployment should be easier when bounds and limitations to network performance are documented.

### 3. Directly modulated system

The directly modulated system is shown in Fig. 3(a). Figures 3(b) and 3(c) show launch signal quality. Initial signal generation was identical to that described for the reflective system. Here however a number of significant differences were required for the inclusion of the baseband component. In order to accommodate the low frequency demands of the baseband signal, a resistive rather than a reactive combining network was necessary, in this case three Pico-second Pulse Labs two way RF splitter/combiners (PSPL 5333-104) were combined to produce a four-way resistive network having the minimum insertion loss of 12 dB. Using the same signal generation set-up as before, and to compensate for this loss, the UWB signal was amplified using a Hittite (HMC392LC) 15 dB gain low-noise amplifier. The LTE and WiMAX signals were increased in level accordingly to preserve the previously determined optimum performance. A 2 Gbps PRBS data stream was then provided by an Anritsu MP1650A pattern generator. In order to remove the high frequency harmonic content of this signal, it was then pre-filtered with a Mini-Circuits 1.92 GHz low pass filter (VLFX-1300) before being passed to the combiner.

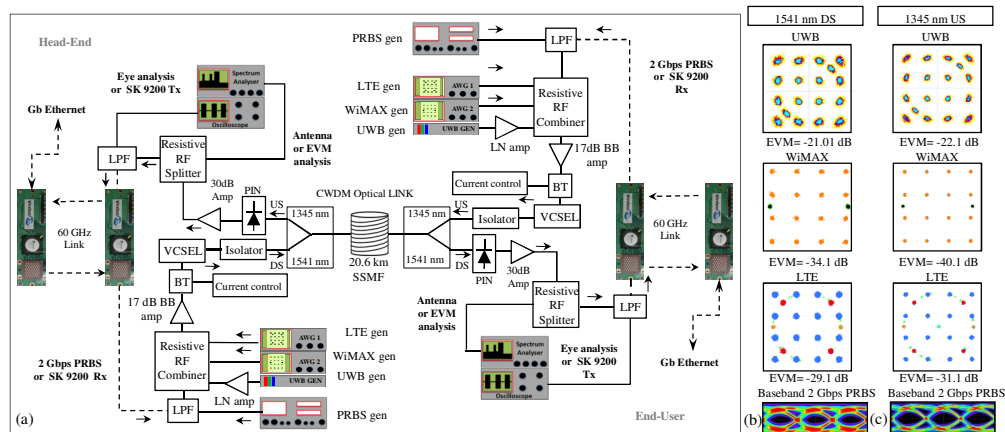


Fig. 3. (a) System diagram showing bidirectional transmission path. Measured EVM, constellations and eye diagram for UWB, WiMAX, LTE and GbE baseband signals in back-to-back configuration (0 km SSMF) for VCSEL bias 10 mA in: (b) 1541 nm DS path and (c) 1345 nm US path

The composite signal was then amplified by 17 dB using an ERA broadband amplifier (WBA1-5-15G28P22) to give peak signal levels of  $-25$  dBm for the baseband, LTE and WiMAX signals and  $-30$  dBm for the UWB signal. At this point, the now complete signal was applied to a  $< 14$  dB return-loss matched 1541 nm VCSEL (Vertilas VL-1550-10G-P2-H4) via a broadband bias-tee (PSPL 5575A) to facilitate the DS optical signal. The US signal generation was identical except for the use of a similarly matched 1345 nm VCSEL (Vertilas VL-1550-10G-P2-H4). Both the 1541nm and 1345nm devices were biased at 10mA. Figures 3(b) and 3(c) are the resulting constellation and eye diagrams of the DS and US signals at 0 km. Figure 4(a) shows the spectrum at the VCSEL input indicating clear separation of the

different formats. Figure 4(b) is the spectrum after the 1541 nm DS VCSEL and Fig. 4(c) is the spectrum after the 1345nm US device. The 2 Gbps PRBS signal imposed the largest total loading at  $-5.1$  dBm compared to UWB at  $-12.2$  dBm total. Evidence of spectral regrowth was clear in the UWB region with the 1541nm VCSEL, in particular, showing signs of producing in/out-band distortion products. Although the imposition of the baseband signal exaggerated this, as shown in Figs. 3(b) and 3(c), clear constellations and eye diagrams were obtained at launch. Here it can be seen that the EVMs for the 1541nm device are inferior to those of the 1345nm device as would be expected. Being in close proximity to the UWB signal, the WiMAX format exhibited the highest vulnerability in these conditions with a 6 dB difference in EVM between the two wavelengths as compared to LTE with a 3 dB difference and UWB with a 1 dB penalty.

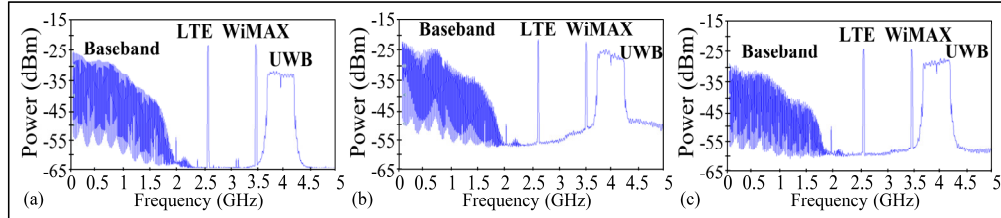


Fig. 4. (a) Spectrum at input to VCSELs. (b) At output of 1541nm DS device. (c) At output of 1345nm US device

It was found necessary to use optical isolators to prevent reflection effects after both DS and US VCSELs (Laser 2000 IS-D-1500-1-1 and IS-D-1300-1-1 respectively) before connection to the CWDM multiplexers (Laser 2000 LAS-10-086) and on to 20.6 km SSMF). After passage through the fiber, a 10 GHz bandwidth photodiode with integral 20 dB gain amplifier (Discovery DSC-R402AC) was used for optical to electrical conversion. This was followed by a further 30 dB wide-band gain-block (ERA WBA1-5-15G28P22). The resulting signal was passed to a two-way resistive splitter (PSPL 5333-104) one output of which was connected to either a UWB antenna (for onward transmission) or constellation/EVM analysis. The second splitter output was then passed through a further 1.92 GHz low-pass filter this time to remove unwanted wireless signal interference from the baseband component and onward to a 50 GHz sampling oscilloscope (LeCroy NRO 9000) for eye diagram observation. A real-time analyzer (Tektronix DPO 71254) provided UWB constellation processing whilst a signal-processing spectrum analyzer (Agilent EXA N9010) rendered LTE/WiMAX constellations and provided EVM measurements. Both US and DS paths are identical allowing unimpeded fully duplex operation between the customer premises and the intermediate (head end) node.

#### 4. Reflective system performance

From the outset of the experimental trials, significant noise products became apparent in the 1500 nm US (reflected) optical path. This indicated severe stimulated Brillouin scattering that increased in severity up to launch powers of  $+14$  dBm that are required to achieve the required range. Baseband transmission in the desired 0 GHz to 2 GHz region would therefore be seriously inhibited by this effect and so cannot be considered viable. Figure 5(a) shows the received RF spectrum, the SBS generated peak which dominated the lower end of the range, increasing in amplitude with the range/power requirement of the R-EAT. Figure 5(b) shows the corresponding optical spectra the dashed trace indicates the spectrum of the directly measured laser, the lower solid trace is the unmodulated, reflected signal from the R-EAT. Due to the SBS effect, part of the light is backscattered at a shifted optical frequency and double-sideband development is observed at around the classical 10.9 GHz. This translates to severe base-band and band-pass electrical noise from 10.9 to 21.8 GHz. The noise-free spectral zone shown in Fig. 5(c) still allowed the transmission of OFDM based signals suitable for LTE at 2.6 GHz, WiMAX at 3.5 GHz and UWB from 3.1 to 10.6 GHz.

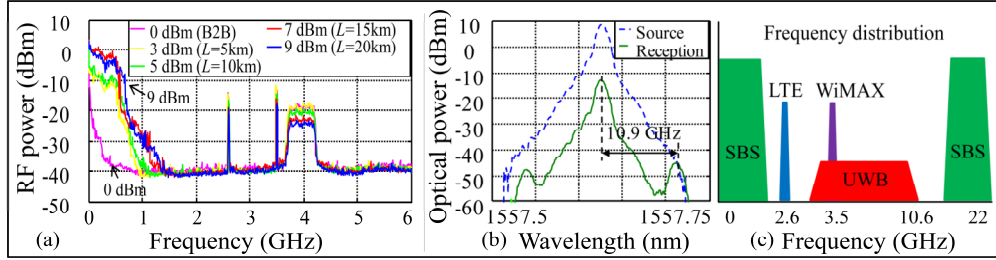


Fig. 5. (a) Frequency spectrum showing SBS. (b) Optical spectrum showing sidebands. (c) Positioning of RF spectrum with respect to SBS peaks

The performance of the R-EAT was now assessed using the triple format OFDM wireless signal up to the target distance of 20 km. Initially the absorbed 1300 nm path was evaluated. Figure 6(a) shows the EVM values of all three formats together with the standards thresholds measured “back-to-back” (i.e.  $L = 0$  km). It can be seen that the EVM reduced as the launch power was increased. The threshold for successful multi-format recovery was 5 dBm, limited by the performance of the WiMAX signal; the first to fall below the standards threshold. Similarly, Fig. 6(b) shows the EVM vs. length for the optimum launch power in each case (up to the 14.5 dBm available). It can be seen that the WiMAX format reached the standards limit after 25.3 km. Figure 6(c) shows the received constellations at 20.2 km and Fig. 6(d) at 25.3 km. At this distance, WiMAX did not meet the limit of  $-24.43$  dB EVM, but with the use of error correction, this situation could be rectified.

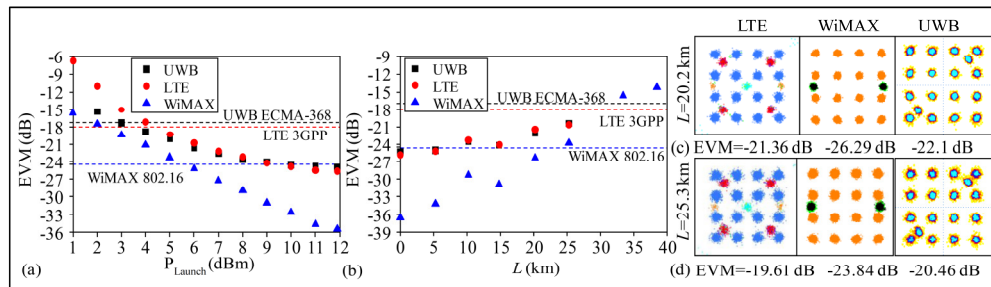


Fig. 6. (a) Measured EVM of LTE, WiMAX and UWB on the absorbed path (1345 nm) vs. optical launch power. (b) EVM vs. length and received constellations and EVM after: (c) 20.2 km, (d) 25.3 km

In the case of the 1541 nm reflected path, Fig. 7(a) shows that optimal EVM of all three wireless formats was achieved at a launch power of  $-1$  dBm in a back-to-back (0km) configuration. Due to saturation of the electrical amplifiers that follow the photodiode with increasing optical power, the EVM was degraded beyond this point. Figure 7(b) shows the EVM at differing fiber lengths obtained using an optimal launch power in each case. It can be seen that whilst fiber losses at the 1500 nm wavelength are, as expected lower than at 1300 nm, the reflected 1500 nm signal has to travel twice the distance. The overall effect being that for all formats to be standards compliant, range is limited to 15 km. Figure 7(c) shows the resulting constellations obtained at this point. At 20.2 km, WiMAX again falls below the standards requirement, however, at this range the signal information could again probably be recovered using error correction as there is minimal inter-symbol collision in the constellation as shown in Fig. 7(d).

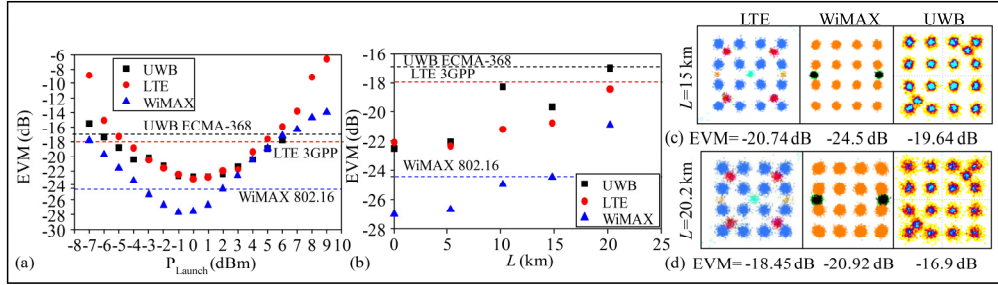


Fig. 7. (a). Measured EVM of LTE, WiMAX and UWB on the reflected path (1550 nm) vs. optical launch power. (b) EVM vs. fiber length and constellations and EVM after (c) 15 km, (d) 20.2 km

As can be seen from Figs. 5(a) and 5(c) the chosen wireless formats fall between the frequency spectral components generated by scattering and so are out of band to any direct effects. Signal degradation shown between Fig. 6 and Fig. 7 is due to device saturation at one extreme and signal to noise ratio effects at the other.

### 5. Direct modulation system performance

Overall system performance was initially assessed at the target distance of 20.6 km with both the DS 1541 nm and US 1345 nm VCSELs biased at 10 mA. This represented optical launch powers of  $-3.6$  dBm and  $-2.8$  dBm respectively. Under these conditions, all three formats were found to meet standards compliance in both directions and clear and open 2 Gbit/s eye diagrams were obtained. The performance of the 1541 nm DS path is shown in Fig. 8. As before, simultaneous presence of all four formats was monitored using the spectrogram technique, here the baseband signal is clearly visible to the left of the spectrogram plot with the spectral regrowth attributed to the UWB pulses visible to the right. Also shown in Figs. 8(b)–8(d) are the constellations relating to the three wireless formats and (e) the received eye diagrams at bias currents of 4 mA, 7 mA and 10 mA.

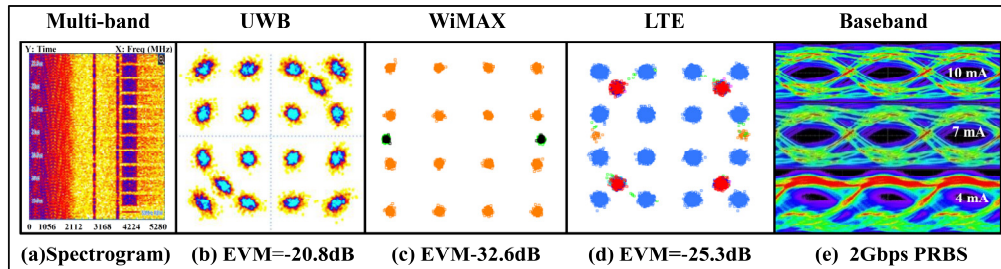


Fig. 8. (a) Spectrogram and signal constellations for (b) UWB, (c) WiMAX, (d) LTE measured after 20.6 km SSMF with 10 mA VCSEL bias and (e) baseband eye diagram variation across 4-10 mA bias range for the 1541 nm DS path

Figure 9 shows the corresponding results for the 1345 nm US path indicating the full duplex transmission capability of the system. As would be expected from the launch conditions, both the EVM plots of the wireless formats and the baseband eye diagrams are superior to that of the DS path. Also the spectrogram plot indicates the absence of any spectral regrowth products.

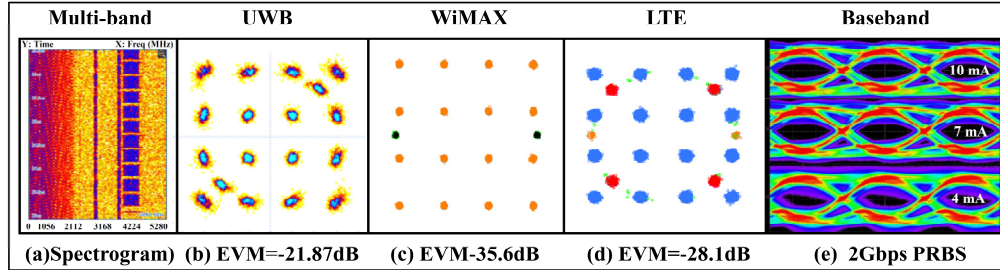


Fig. 9. (a) Spectrogram and signal constellations for (b) UWB, (c) WiMAX, (d) LTE measured after 20.6 km SSMF with 10 mA VCSEL bias and (e) baseband eye diagram variation across 4-10 mA bias range for the 1345 nm US path

In Figs. 10(a)-10(c), EVM variation with 1541 nm received power level is plotted for each signal UWB, WiMAX and LTE respectively. All standards are indicated as before and are compliant above  $\sim -11$  dBm or  $\sim 9$  mA VCSEL bias. Figures 11(a)-11(c) shows, finally, that the 1345 nm US path also offers complete wireless signal integrity at these levels.

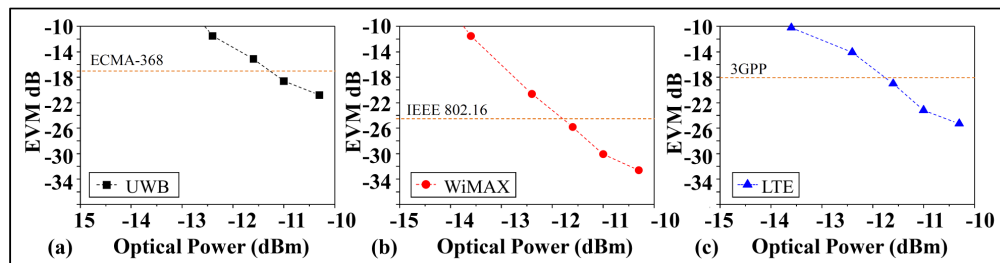


Fig. 10. EVM standard compliance with 1541 nm DS path received power after 20.6 km SSMF for: (a) UWB, (b) WiMAX and (c) LTE

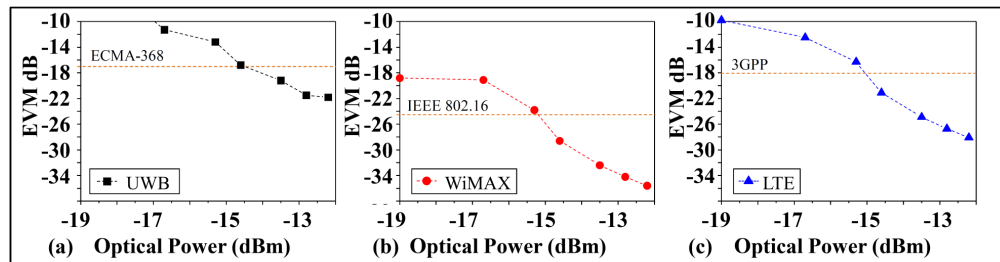


Fig. 11. EVM standard compliance with 1345 nm US path received power after 20.6 km SSMF for: (a) UWB, (b) WiMAX and (c) LTE

## 6. Conclusions

Fiber-to-the-home networks have the capacity to deliver multiple services to the domestic end user in their native format. In doing so, greatly simplified customer premises equipment results since standard commercial devices can then be utilized. Such systems require bi-directional links that necessitate the deployment of costly and inappropriate lasers in the domestic environment. Two, low power, optical solutions have been assessed that serve to interface the customer premises to the main metro network and their performance attributes compared. The principal advantage of the reflective network is that allows both US and DS lasers to be remotely situated away from the user premises with clear implications for system reliability and installation costs. Performance however is inhibited in several key areas. Due to a common RF port, the device is only suitable for half duplex operation, still requiring the addition of external switching. Range is limited to around 15 km due is some part to the US

(reflected) path travelling twice the system range. Using forward error correction this may be extended to a useable range of 20 km. Within these limitations the system delivers multiple wireless services but suffers with inherent generation of SBS that prevents the transmission of baseband signals. By permitting the use of a directly-modulated VCSEL device at the end user premises a cost effective, full-duplex CWDM system becomes a practical proposition. Evaluation of this approach established that a target distance of 20 km could be achieved without the need for any further remedial processing in order to comply with the relevant standards. Without the presence of SBS, the three wireless formats and a 2 Gbps baseband signal were successfully transmitted simultaneously. This opens the possibility of Gigabit Ethernet access to in-building Picocell networking at 60 GHz.

### **Acknowledgments**

This work has been partly funded by FP7 ICT-4-249142 FIVER project. M. Morant's work is supported by the Spanish FPU MEC grant AP2007-01413. The EUROFOS NoE is also acknowledged.